follows. Cp: C-C, 1.42 Å; C-H, 1.09 Å; Cp(centroid)-U, 2.54 Å; Cp(centroid)-U-Cp(centroid), 109.47°. NPH_3: N-P, 1.60 Å; P-H, 1.42 Å; H-P-H, 109.47°. NPh: N-C, 1.34 Å; C-C, 1.40 Å; C-H, 1.09 Å; Ph, idealized hexagon. $NCHCHPH_3$: N-C, 1.34 Å; C-C, 1.39 Å; C-P, 1.74 Å; P-H, 1.42 Å; N-C-C, 128°; C-C-P, 123°. NH_3, NH_2: N-H, 1.02 Å. OPH_3: O-P, 1.492 Å. OH_2: O-H, 1.0 Å; H-O-H, 100°. $OCHCHPH_3$: O-C, 1.33 Å; C-C, 1.40 Å; C-P, 1.71 Å; O-C-C, 118.5°. OCH_3: O-C, 1.43 Å. All the U-N and U-O distances are fixed at 2.06 Å.

Acknowledgment. The support of this work at the University of Hawaii by the National Science Foundation, Grant CHE 85-19289 (J.W.G. and R.E.C.) and by the donors of the Petroleum Research Fund, administered by the American Chemical Society (R.E.C. and J.W.G.), is gratefully acknowledged. Collaboration between Osaka University and the University of Hawaii was supported by the US/Japan Cooperative Science Program, National Science Foundation Grant INT 84-12205 (J.W.G. and R.E.C.), and a grant from the Japan Society for the Promotion of Science (K.T. and A.N.). The support of the Alexander von Humboldt Foundation through a Feodor Lynen Fellowship (F.E.) is also gratefully acknowledged.

Registry No. $LiNPPh_3$, 13916-35-3; Cp_3UNPPh_3, 112219-51-9; Cp_3UCl, 1284-81-7; $Cp_3ThNPPh_3$, 112196-30-2; Cp_3ThCl, 1284-82-8; Cp_3UNPH_3, 112196-31-3; Cp_3UNPh, 112196-32-4; $Cp_3UNCHCHPH_3$, 112196-33-5; Cp_3UNH_2, 112196-34-6; $Cp_3UNH_3^+$, 112196-35-7; Cp_3UOPH_3, 112196-36-8; Cp_3UOH_2, 112196-37-9; $Cp_3UOCHCHPH_3$, 112196-38-0; Cp_3UOCH_3, 1284-84-0.

Supplementary Material Available: Table III, positional and thermal parameters for the hydrogen atoms of Cp_3UNPPh_3 (1 page); Table IV, observed and calculated structure factors for Cp_3UNPPh_3 (14 pages). Ordering information is given on any current masthead page.

Preparation, Reactivity, Hydroformylation Catalysis, and Structural Studies of the Early Transition Metal/Late Transition Metal Heterobimetallic Complexes $Cp_2M(\mu\text{-}PR_2)_2M'H(CO)PPh_3$ (M = Zr, Hf; M' = Rh, Ir)

Lucio Gelmini and Douglas W. Stephan*

Department of Chemistry and Biochemistry, University of Windsor, Windsor, Ontario, Canada N9B 3P4

Received June 29, 1987

A series of complexes of the form $Cp_2M(\mu\text{-}PR_2)_2M'H(CO)PPh_3$ (1) have been prepared. Complexes 2-7 [M = Zr, R = Ph, M' = Rh (2); M' = Ir (3); R = Cy, M' = Rh (4); M = Hf, R = Ph, M' = Ir (5); M' = Rh (6); R = Cy (7)] have been characterized by IR, UV-vis, $^{31}P\{^1H\}$ NMR, and ^1H NMR spectroscopy. Compound 2 crystallizes in the monoclinic space group $P2_1/n$ with a = 16.398 (3) Å, b = 20.953 (6) Å, c = 13.560 (4) Å, β = 103.48 (2)°, and Z = 4. The hafnium analogue of 2 (i.e., 6) is isostructural to 2 and also crystallizes in the space group $P2_1/n$ with a = 16.372 (2) Å, b = 20.931 (4) Å, c = 13.588 (3) Å, β = 103.68 (1)°, and Z = 4. Substitution reactions involving replacement of the phosphine bound to Rh in 2 with either more basic phosphines (PEt_3, PCy_3) or CO have been studied. The substitution products $Cp_2Zr(\mu\text{-}PPh_2)_2RhH(CO)PR_3$ [R = Et (8), R = Cy (9), and $Cp_2Zr(\mu\text{-}PPh_2)_2RhH(CO)_2$ (10)] have been characterized. Compound 2 is a catalyst precursor for the catalysis of the hydroformylation of 1-hexene. Although the rate of catalysis is slower for this heterobimetallic catalyst than for related monometallic Rh species, the selectivity for terminal aldehydes is significantly greater. Aspects of the mechanism of catalysis are discussed in light of the structural and chemical data, and the role of the early metal in this chemistry is considered.

Introduction

Heterobimetallic complexes have been the subject of numerous recent studies.[1-39] In particular, interest has focused on the complexes containing early, electron-deficient and late, electron-rich metal centers. Such systems

(1) Casey, C. P.; Jordan, R. F.; Rheingold, A. L. *J. Am. Chem. Soc.* **1983**, *105*, 665 and references therein.
(2) Ho, S. C. H.; Strauss, D. A.; Armantrout, J.; Schafer, W. P.; Grubbs, R. H. *J. Am. Chem. Soc.* **1984**, *106*, 2210.
(3) Besecker, C. J.; Day, V. W.; Klemperer, W. G.; Thompson, M. R. *J. Am. Chem. Soc.* **1984**, *106*, 4125.
(4) McLain, S. J. *J. Am. Chem. Soc.* **1983**, *105*, 6355.
(5) Butts, S. B.; Strauss, S. H.; Holt, E. M.; Stimson, R. E.; Alcock, N. W.; Shriver, D. F. *J. Am. Chem. Soc.* **1980**, *102*, 5093.
(6) Bianchini, C.; Meli, A. *J. Am. Chem. Soc.* **1984**, *106*, 2698.
(7) Ritchey, J. M.; Zozulin, A. J.; Wrobleski, D. A.; Ryan, R. R.; Wasserman, H. J.; Moody, D. C.; Paine, R. T. *J. Am. Chem. Soc.* **1985**, *107*, 501.
(8) Martin, B. D.; Matchett, S. A.; Norton, J. R.; Anderson, O. P. *J. Am. Chem. Soc.* **1985**, *107*, 7952.
(9) Sartain, W. J.; Selegue, J. P. *J. Am. Chem. Soc.* **1985**, *107*, 5818.
(10) Casey, C. P.; Palermo, R. E.; Jordan, R. F.; Rheingold, A. L. *J. Am. Chem. Soc.* **1985**, *107*, 4597.
(11) Casey, C. P.; Palermo, R. E.; Rheingold, A. L. *J. Am. Chem. Soc.* **1986**, *108*, 549.
(12) Ortiz, J. V. *J. Am. Chem. Soc.* **1986**, *108*, 550.
(13) Tso, C. T.; Cutler, A. R. *J. Am. Chem. Soc.* **1986**, *108*, 6069.
(14) Casey, C. P.; Jordan, R. F.; Rheingold, A. L. *Organometallics* **1984**, *3*, 504.
(15) Barger, P. T.; Bercaw, J. E. *Organometallics* **1984**, *3*, 278.
(16) Mayer, J. M; Calabrese, J. C. *Organometallics* **1984**, *3*, 1292.
(17) Choukroun, R.; Gervais, D.; Jaud, J.; Kalck, P.; Senocq, F. *Organometallics* **1986**, *5*, 67.
(18) Ferguson, G. S.; Wolczanski, P. T. *Organometallics* **1985**, *4*, 1601.
(19) Casey, C. P.; Nief, F. *Organometallics* **1985**, *4*, 1218.
(20) Ruffing, C. J.; Rauchfuss, T. B. *Organometallics* **1985**, *4*, 524.
(21) Khasnis, D. V.; Bozec, H. L.; Dixneuf, P. H. *Organometallics* **1986**, *5*, 1772.
(22) Targos, T. S.; Rosen, R. P.; Whittle, R. R.; Geoffroy, G. L. *Inorg. Chem.* **1985**, *24*, 1375.
(23) Baker, R. T.; Tulip, T. H.; Wreford, S. S. *Inorg. Chem.* **1985**, *24*, 1379.
(24) Schumann, H.; Albrecht I.; Hahn, E. *Inorg. Chem.* **1985**, *11*, 985.
(25) Choukroun, R.; Gervais, D. *J. Organomet. Chem.* **1984**, *266*, C37.
(26) Erker, G.; Dorf, U.; Kruger, C.; Tsay, Y. H. *Organometallics* **1987**, *6*, 680.

0276-7333/88/2307-0849$01.50/0

offer the potential of cooperative activation of carbon oxide substrates by the two constituent metals. Lewis acidic, early metals are capable of interacting with the oxygen of a substrate which is carbon bound to the later metal atom. This type of Lewis acid interaction with early metals has been observed in the reactions of group 9 metal carbonylates with group 4 metallocene alkyls.[1] More recently, Choukroun and co-workers observed hydroformylation catalysis by a Zr–Rh heterobimetallic species in which enhanced activity was attributed to Lewis acid activation of CO by the Zr.[17,25]

In our attempt to develop the chemistry of heterobimetallic complexes, our research focused initially on the establishment of convenient synthetic routes to such species.[31-39] The approach has been to utilize functionalized early-transition-metal complexes as metalloligands to bind later transition metal atoms. We have previously described heterobimetallic systems based on the metalloligands $Cp_2Ti(S(CH_2)_nPPh_2)_2$ (n = 2, 3),[35,37] $Cp_2Ti(SEt)_2$,[36] and $Cp_2Zr(PPh_2)_2$.[31-33] Other workers have described related complexes derived from $CpZr(OCH_2PPh_2)_3$[18,28] and $Cp_2M(PR_2)_2$ (M = Zr, Hf; R = Ph, Cy).[23] In the derived heterobimetallics, chemical, theoretical,[37] and structural data suggest the presence of dative interactions between the electron-rich and electron-deficient metal centers. Such interactions may be the cause of the "butterfly" type geometry of the MP_2M' core seen in several of these complexes. To further investigate the chemistry of early/late heterobimetallics, we have prepared a series of phosphido-bridged species of the form $Cp_2M(\mu\text{-}PR_2)_2M'H(CO)PPh_3$ (1). Complexes **2–7** [M = Zr, R = Ph, M′ = Rh (**2**);

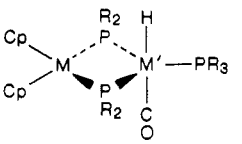

1

M′ = Ir (**3**); R = Cy, M′ = Rh (**4**); M = Hf, R = Ph, M′ = Ir (**5**); M′ = Rh (**6**); R = Cy (**7**)] have been prepared and spectroscopically characterized. Crystallographic data for **2** and **6** are presented. The reactivity of **2** with basic phosphines, CO, hexene, and H_2 is described. The catalysis of the hydroformylation of 1-hexene using **2** as the catalyst precursor has been examined. Mechanistic aspects of the catalysis are discussed in light of the structural and chemical data, and the role of the early transition metal in this chemistry is considered.

Experimental Section

All preparations were done under an atmosphere of dry, O_2-free N_2. Solvents were reagent grade, distilled from the appropriate drying agents under N_2, and degassed by the freeze–thaw method at least three times prior to use. ^1H NMR spectra were recorded on a Bruker AC-300 spectrometer, using the trace of protonated solvent as the reference. The chemical shifts are reported in parts per million relative to $Si(CH_3)_4$ for the ^1H NMR data. ^{31}P and $^{31}P\{^1H\}$ NMR spectra were recorded on a Bruker AC-200 spectrometer. ^{31}P NMR chemical shifts are reported in parts per million relative to external 85% H_3PO_4. UV–vis data were recorded on a Shimadzu 240 spectrometer or a Hewlett-Packard 8451A diode-array spectrophotometer. Combustion analyses were performed by Spang Laboratories, Eagle Harbor, MI. $Cp_2Zr(PPh_2)_2$, $Cp_2Hf(PPh_2)_2$, $Cp_2Zr(PCy_2)_2$, $Cp_2Hf(PCy_2)_2$, $RhH(CO)(PPh_3)_3$, and $IrH(CO)(PPh_3)_3$ were prepared by literature methods.[33,40-42]

Preparation of $Cp_2M(\mu\text{-}PR_2)_2M'H(CO)PPh_3$ [M = Zr, R = Ph, M′ = Rh (2); M′ = Ir (3); R = Cy, M′ = Rh (4); M = Hf, R = Ph, M′ = Ir (5); M′ = Rh (6); R = Cy (7)]. These compounds were prepared by the following procedure with the appropriate changes in the starting materials. Thus, only a sample preparation is given. A suspension of 200 mg (0.34 mmol) of $Cp_2Zr(PPh_2)_2$ in 10 mL of diethyl ether was added to a suspension of 310 mg (0.34 mmol) of $RhH(CO)(PPh_3)_3$ in 15 mL of n-pentane and 5 mL of THF. The mixture was stirred for 8 h at 25 °C. The product was isolated by filtration, and the solid was washed with three 5-mL portions of both diethyl ether and acetone. In the cases where R = Cy, solubility of the heterobimetallic species precluded isolation by precipitation. In these cases the products were characterized by spectroscopic study of the reaction mixtures. **2**: 215 mg (65%); ^1H NMR (C_6D_6) δ 6.9–7.9 (m, 35 H), 5.25 (s, 5 H), 4.97 (s, 5 H), −12.49 (d of d of t, 1 H, $|J(H\text{–}PR_2)|$ = 20 Hz, $|J(H\text{–}PR_3)|$ = 8 Hz, $|J(H\text{–}Rh)|$ = 3 Hz); $^{31}P\{^1H\}$ NMR (THF) δ 122.9 (d of d, 2 P, $|J(P\text{–}P)|$ = 14 Hz, $|J(P\text{–}Rh)|$ = 99 Hz), 41.6 (d of t, 1 P, $|J(P\text{–}Rh)|$ = 140 Hz); UV–vis (THF; λ, nm (ϵ, M^{-1} cm^{-1})) 278 (500), 376 (500); IR (KBr, cm^{-1}) 2017 (Rh–H), 1934 (C–O). Anal. Calcd for $C_{53}H_{46}OP_3RhZr$: C, 64.56; H, 4.70. Found: C, 64.93; H, 4.77. **3**: 255 mg (70%); ^1H NMR (C_6D_6) δ 6.9–7.9 (m, 35 H), 5.11 (s, 5 H), 4.93 (s, 5 H), −13.49 (d of t, 1 H, $|J(H\text{–}PR_2)|$ = 19 Hz, $|J(H\text{–}PR_3)|$ = 19 Hz); $^{31}P\{^1H\}$ NMR (THF) δ 91.3 (d, 2 P, $|J(P\text{–}P)|$ = 7 Hz), 8.6 (t, 1 P); UV–vis (THF; λ, nm (ϵ, M^{-1} cm^{-1})) 284 (1200), 370 (800); IR (KBr, cm^{-1}) 2099 (Ir–H), 1940 (C–O). Anal. Calcd for $C_{53}H_{46}IrOP_3Zr$: C, 59.20; H, 4.31. Found: C, 59.52; H, 4.58. **4**: ^1H NMR (C_6D_6) δ 6.9–7.9 (m, 15 H), 5.56 (s, 5 H), 5.40 (s, 5 H), 1.0–2.0 (m, 44 H), −13.80 (d of d of t, 1 H, $|J(H\text{–}PR_2)|$ = 26 Hz, $|J(H\text{–}PR_3)|$ = 8 Hz, $|J(H\text{–}Rh)|$ = 4 Hz); $^{31}P\{H\}$ NMR (THF) δ 131.2 (d of d, 2 P, $|J(P\text{–}P)|$ = 19 Hz, $|J(P\text{–}Rh)|$ = 86 Hz), 44.5 (d of d of t, 1 P, $|J(P\text{–}RH)|$ = 137 Hz); IR (KBr, cm^{-1}) 2019 (Rh–H), 1957 (C–O). **5**: 255 mg (70%); ^1H NMR (C_6D_6) δ 6.9–7.9 (m, 35 H), 5.06 (s, 5 H), 4.89 (s, 5 H), −13.47 (d of t, 1 H, $|J(H\text{–}PR_2)|$ = 19 Hz, $|J(H\text{–}PR_3)|$ = 19 Hz); $^{31}P\{^1H\}$ NMR (THF) δ 82.5 (d, 2 P, $|J(P\text{–}P)|$ = 12 Hz), 10.5 (t, 1 P); UV–vis (THF; λ, nm (ϵ, M^{-1} cm^{-1})) 283 (800), 372 (600); IR (KBr, cm^{-1}) 2110 (Ir–H), 1936 (C–O). Anal. Calcd for $C_{53}H_{46}HfIrOP_3$: C, 54.75; H, 3.99. found: C, 54.32; H, 4.03. **6**: 335 mg (70%); ^1H NMR (C_6D_6) δ 6.9–7.9 (m, 35 H), 5.17 (s, 5 H), 4.93 (s, 5 H), −12.41 (d of d of t, 1 H, $|J(H\text{–}PR_2)|$ = 21 Hz, $|J(H\text{–}PR_3)|$ = 9 Hz, $|J(H\text{–}Rh)|$ = 2.5 Hz); $^{31}P\{^1H\}$ NMR (THF) δ 114.9 (d of d, 2 P, $|J(P\text{–}P)|$ = 16 Hz, $|J(P\text{–}Rh)|$ = 97 Hz), 42.9 (d of t, 1 P, $|J(P\text{–}Rh)|$ = 140 Hz); UV–vis (THF; λ, nm (ϵ, M^{-1} cm^{-1})) 274 (800), 364 (800); IR (KBr, cm^{-1}) 2031 (Rh–H), 1933 (C–O). Anal. Calcd for $C_{53}H_{46}HfOP_3Rh$: C, 59.31; H, 4.32. Found: C, 59.55; H, 4.76. **7**: ^1H NMR (C_6D_6) δ 6.9–7.9 (m, 15 H), 5.53 (s, 5 H), 5.38 (s, 5 H), 1.0–2.0 (m, 44 H), −13.60 (d of d of t, 1 H, $|J(H\text{–}PR_2)|$ = 24 Hz, $|J(H\text{–}P)|$ = 8 Hz, $|J(H\text{–}Rh)|$ = 4 Hz); $^{31}P\{^1H\}$ NMR (THF) δ 116.9 (d of d, 2 P, $|J(P\text{–}P)|$ = 21 Hz, $|J(P\text{–}Rh)|$ = 83 Hz), 45.9 (d of d of t, 1 P, $|J(P\text{–}Rh)|$ = 136 Hz); IR (KBr, cm^{-1}) 2087 (Rh–H), 1938 (C–O).

Formation of $Cp_2Zr(\mu\text{-}PPh_2)_2RhH(CO)PR_3$ [R = Et (8); R = Cy (9)]. To a solution of 100 mg (0.10 mmol) of **2** in 5 mL of THF was added a stoichiometric amount of phosphine (PEt_3 or PCy_3). The solution was stirred for 10 min. Addition of n-hexane resulted in the precipitation of an orange-yellow solid that was

(27) Mashima, K.; Jyodoi, K.; Ohyoshi, A.; Takaya, H. *Organometallics* **1987**, *6*, 885.
(28) Ferguson, G. S.; Wolczanski, P. T. *J. Am. Chem. Soc.* **1986**, *108*, 8293.
(29) Tso, C. T.; Cutler, A. R. *J. Am. Chem. Soc.* **1986**, *108*, 6069.
(30) Park, J. W.; Mackenzie, P. B.; Schaefer, W. P.; Grubb, R. H. *J. Am. Chem. Soc.* **1986**, *108*, 6402.
(31) Gelmini, L.; Matassa, L. C.; Stephan, D. W. *Inorg. Chem.* **1985**, *24*, 2585.
(32) Gelmini, L.; Stephan, D. W. *Inorg. Chem.* **1986**, *25*, 1222.
(33) Gelmini, L.; Stephan, D. W. *Inorg. Chim. Acta* **1986**, *111*, L17.
(34) Loeb, S. J.; Taylor, H. A.; Gelmini, L.; Stephan, D. W. *Inorg. Chem.* **1986**, *25*, 1977.
(35) White, G. S.; Stephan, D. W. *Inorg. Chem.* **1985**, *24*, 1499.
(36) Wark, T. A.; Stephan, D. W. *Inorg. Chem.* **1987**, *26*, 363.
(37) White, G. S.; Stephan, D. W. *Organometallics* **1987**, *6*, 2169.
(38) Wark, T. A.; White, G. S.; Tse, J. S.; Stephan, D. W., unpublished results.
(39) Gelmini, L.; Stephan, D. W. *Organometallics* **1987**, *6*, 1515.
(40) Wade, S. R.; Wallbridge, M. G. H.; Willey, G. R. *J. Chem. Soc., Dalton Trans.* **1983**, 2555.
(41) Uttley, M. F.; Ahmad, N.; Levison, J. J.; Robinson, S. D. *Inorg. Synth.* **1974**, *15*, 59.
(42) Wilkinson, G. *Inorg. Synth.* **1972**, *13*, 126.

Table I. Crystallographic Parameters

	2	6
formula	$C_{53}H_{46}P_3OZrRh$	$C_{53}H_{46}P_3OHfRh$
cryst color, form	yellow blocks	yellow blocks
cryst syst	monoclinic	monoclinic
space group	$P2_1/n$	$P2_1/n$
a (Å)	16.398 (3)	16.372 (2)
b (Å)	20.953 (6)	20.931 (4)
c (Å)	13.560 (4)	13.588 (3)
β (deg)	103.48 (2)	103.68 (1)
V (Å^3)	4531 (2)	4524 (1)
D	1.45	1.57
Z	4	4
cryst dimens (mm)	0.4 × 0.4 × 0.5	0.3 × 0.3 × 0.4
abs coeff μ (cm^{-1})	6.53	26.43
radiatn λ, Å	Mo Kα (0.71069)	Mo Kα (0.71069)
temp (°C)	24	24
scan speed (deg/min)	2.0–5.0	2.0–5.0
scan range (deg)	1.0 below Kα_1 1.1 above Kα_2	1.0 below Kα_1 1.0 above Kα_2
bkgd/scan time ratio	0.5	0.5
unique data	4652	6387
data $F_o^2 > 3\sigma(F_o^2)$	3494	4662
no. of variables	272	272
R (%)	4.08	5.38
R_w (%)	4.80	5.61
max Δ/σ in final cycle	0.001	0.004
largest residual electron density (e/Å^3)	0.67	2.45
atom associated with residual density	C15–C16	Hf

found to contain a mixture of **2** and the phosphine-substituted complex **8** or **9**. Equilibrium constants were determined by integration of the ^{31}P NMR spectra. **8**: ^1H NMR (C_6D_6) δ 6.9–8.2 (m, 20 H), 5.16 (s, 5 H), 4.83 (s, 5 H), −13.18 (d of d of t, 1 H, $|J(H-PR_2)|$ = 21 Hz, $|J(H-PR_3)|$ = 12 Hz, $|J(H-Rh)|$ = 4 Hz); $^{31}P\{^1H\}$ NMR (THF) δ 136.1 (d of d, 2 P, $|J(P-P)|$ = 9 Hz, $|J(P-Rh)|$ = 100 Hz), 25.1 (d of t, 1 P, $|J(P-Rh)|$ = 137 Hz); IR (KBr, cm^{-1}) 2016 (Rh–H), 1922 (C–O). **9**: ^1H NMR (C_6D_6) δ 8.1–7.9 (m, 20 H), 5.34 (s, 5 H), 4.78 (s, 5 H), −13.25 (d of d of t, 1 H, $|J(H-PR_2)|$ = 20 Hz, $|J(H-PR_3)|$ = 10 Hz, $|J(H-Rh)|$ = 4 Hz); $^{31}P\{^1H\}$ NMR (THF) δ 128.0 (d of d, 2 P, $|J(P-P)|$ = 10 Hz, $|J(P-Rh)|$ = 102 Hz), 54.5 (d of t, 1 P, $|J(P-Rh)|$ = 135 Hz); IR (KBr, cm^{-1}) 2017 (Rh–H), 1936 (C–O).

Formation of $Cp_2Zr(\mu\text{-}PPh_2)_2RhH(CO)_2$ (10). CO was bubbled for 12 h through a THF solution (5 mL) containing 100 mg (0.10 mmol) of **2**. The extent of reaction was monitored by NMR and IR spectroscopy. **10**: ^1H NMR (C_6D_6) δ 7.0–8.0 (m, 20 H), 5.06 (s, 10 H), −12.39 (d of t, 1 H, $|J(H-PR_2)|$ = 20 Hz, $|J(H-Rh)|$ = 4 Hz); $^{31}P\{^1H\}$ NMR (THF) δ 128.7 (d, 2 P, $|J(P-Rh)|$ = 92 Hz); IR (KBr, cm^{-1}) 2017 (Rh–H), 1975, 1939 (C–O).

Hydroformylation Catalysis. Each of the reactions employing $RhH(CO)(PPh_3)_3$ or **2** as the catalyst precursor was performed in a similar manner; thus only a general method is described.

A flask charged with 1 g (12 mmol) of 1-hexene, 0.05 mmol of catalyst precursor, and 12.5 mL of benzene was stirred under 1 atm of H_2/CO (50:50) for 100 h. The reaction was monitored by GC and GC–MS at regular intervals during the reaction. In the case of the reaction done in the presence of excess PPh_3, 130 mg (0.5 mmol) of PPh_3 was added.

X-ray Data Collection and Reduction. Yellow crystals of **2** and **6** were obtained by recrystallization from benzene/diethyl ether. Diffraction experiments were performed on a four-circle Syntex $P2_1$ diffractometer with graphite-monochromatized Mo Kα radiation. The initial orientation matrix for each compound was obtained from 15 machine-centered reflections selected from rotation photographs. These data were used to determine the crystal systems. Partial rotation photographs around each axis were consistent with monoclinic crystal systems. Ultimately, 30 high-angle reflections ($22° < 2\theta < 25°$) were used to obtain the final lattice parameters and the orientation matrix for **2**. For **6**, 44 such reflections were used. Machine parameters, crystal data, and data collection parameters are summarized in Table I. The observed extinctions were consistent with the space group $P2_1/n$ for both **2** and **6**. In both cases, $\pm h, +k, +l$ data were collected in one shell ($4.5° < 2\theta < 40°$ for **2** and $4.5° < 2\theta < 45°$ for **6**) and three standard reflections were recorded every 197 reflections. Their intensities showed no statistically significant change over the duration of the data collections. The data were processed by using the SHELX-76 program package on the computing facilities at the University of Windsor. A total of 3494 reflections for **2** and 4662 reflections for **6** with $F_o^2 > 3\sigma(F_o^2)$ were used in their respective refinements. The absorption coefficient for **2** was small (μ = 6.53 cm^{-1}), and thus no absorption correction was applied to the data. For **6**, an empirical absorption correction based on three Ψ scans was applied to the data. This was done by using a locally modified version of the program ABSN.

Structure Solutions and Refinements. Non-hydrogen atomic scattering factors were taken from the literature tabulations.[43,44] For **2**, the Zr atom position was determined by using the heavy-atom (Patterson) method. The remaining non-hydrogen atoms were located from successive difference Fourier map calculations. As **6** is isostructural to **2**, structure solution of **6** was achieved by simply utilizing the positions located for **2** and making the appropriate substitution of Hf for Zr. The refinements were carried out by using full-matrix least-squares techniques on F, minimizing the function $\sum w(|F_o| - |F_c|)^2$ where the weight, w, is defined as $4F_o^2/\sigma^2(F_o^2)$ and F_o and F_c are the observed and calculated structure factor amplitudes, respectively. In the final cycles of refinement the Rh, P, O, carbonyl C, and either Zr or Hf atoms were assigned anisotropic temperature factors. The carbon atoms were described by isotropic thermal parameters. Hydrogen atom positions were calculated and allowed to ride on the carbon to which they are bonded assuming a C–H bond length of 0.95 Å. Hydrogen atom temperature factors were fixed at 1.10 times the isotropic temperature factor of the carbon atom to which they are bonded. The hydride was not located; however, the coordinates were calculated by positioning it trans to the CO moiety at a distance of 1.70 Å from the Rh. In all cases the hydrogen atom contributions were calculated, but not refined. The final values of $R = \sum||F_o| - |F_c|/\sum|F_o||$ and $R_w = (\sum w(|F_o| - |F_c|)^2/\sum wF_o^2)^{1/2}$ are given in Table I. The maximum Δ/σ on any of the parameters in the final cycles of the refinements, and the locations of the largest peaks in the final difference Fourier map calculations are also given in Table I. In either case the residual electron densities were of no chemical significance. The following data are tabulated: positional parameters (Table II); selected bond distances and angles (Table III). Thermal parameters (Table S1), hydrogen atom parameters (Table S2), bond distances and angles associated with the cyclopentadienyl rings (Table S3), and values of $10|F_o|$ and $10|F_c|$ (Table S4) have been deposited as supplementary material.

Results and Discussion

Reactions of zirconocene or hafnocene diphosphides with $MH(CO)(PPh_3)_3$ (M = Rh, Ir) led to formation in good yields (65–75%) of the yellow complexes formulated as $Cp_2M(\mu\text{-}PR_2)_2M'H(CO)PPh_3$ (**1**). This reaction is general for M = Zr or Hf, R = Ph or Cy, and M′ = Rh or Ir, yielding complexes **2–7**. The derived complexes are air-stable in the solid state, unlike the very air-sensitive, early metal diphosphides. Analytical, IR, and ^1H and ^{31}P NMR data as well as the results from two X-ray crystallographic studies (vide infra) were all consistent with these formulations.

The $^{31}P\{^1H\}$ NMR spectra of these compounds show two sets of resonances. For the Ir complexes, a doublet in the range 90–120 ppm is attributed to the phosphorus atoms of bridging phosphido groups. A triplet observed at about 5–15 ppm is attributed to the phosphorus atom of the phosphine group bound to the Ir. For the Rh complexes, these signals are split again by ^{103}Rh yielding the corre-

(43) (a) Cromer, D. T.; Mann, J. B. *Acta Crystallogr., Sect. A: Cryst. Phys., Diffr., Theor. Gen. Crystallogr.* **1968**, *A24*, 324. (b) Cromer, D. T.; Mann, J. B. *Acta Crystallogr. Sect. A: Cryst. Phys., Diffr., Theor. Gen. Crystallogr.* **1968**, *A24*, 390.

(44) Cromer, D. T.; Waber, J. T. *International Tables for X-ray Crystallography*; Kynoch: Birmingham, England, 1974.

Table II. Positional Parameters[a]

atom	x	y	z	atom	x	y	z
			Molecule 2				
Rh	−726 (1)	2565 (1)	1678 (1)	Zr	−1390 (1)	1306 (1)	2154 (1)
P1	−468 (1)	3548 (1)	990 (2)	P2	−544 (1)	1658 (1)	781 (2)
P3	−1570 (1)	2497 (1)	2830 (2)	O	931 (4)	2471 (3)	3255 (5)
C	309 (6)	2515 (3)	2651 (7)	C1	86 (5)	1000 (4)	3087 (6)
C2	−265 (5)	1293 (4)	3800 (6)	C3	−933 (6)	909 (4)	3941 (7)
C4	−985 (6)	374 (5)	3339 (7)	C5	−356 (5)	435 (4)	2781 (7)
C6	−2972 (5)	1355 (4)	1636 (6)	C7	−2755 (5)	743 (4)	2018 (7)
C8	−2354 (5)	439 (5)	1336 (6)	C9	−2317 (5)	845 (4)	572 (7)
C10	−2692 (5)	1425 (4)	740 (6)	C11	−53 (5)	4157 (4)	1927 (6)
C12	690 (5)	4066 (4)	2625 (6)	C13	987 (6)	4498 (5)	3402 (7)
C14	574 (7)	5026 (5)	3475 (8)	C15	−150 (8)	5163 (7)	2764 (10)
C16	−461 (6)	4728 (5)	1984 (8)	C21	322 (5)	3542 (4)	223 (6)
C22	274 (5)	3062 (4)	−495 (6)	C23	878 (6)	3018 (5)	−1064 (7)
C24	1522 (6)	3446 (4)	−908 (7)	C25	1564 (6)	3930 (5)	−244 (7)
C26	961 (5)	3991 (4)	335 (7)	C31	−1352 (5)	3949 (4)	142 (6)
C32	−2113 (5)	3971 (4)	426 (7)	C33	−2810 (6)	4270 (5)	−178 (7)
C34	−2744 (6)	4532 (5)	−1077 (8)	C35	−2012 (6)	4515 (5)	−1376 (8)
C36	−1299 (6)	4230 (4)	−764 (6)	C41	−1039 (4)	1612 (4)	−585 (6)
C42	−827 (5)	1143 (4)	−1202 (6)	C43	−1259 (6)	1072 (5)	−2204 (7)
C44	−1898 (6)	1455 (5)	−2600 (7)	C45	−2124 (6)	1948 (5)	−2031 (7)
C46	−1687 (5)	2014 (4)	−1026 (7)	C51	520 (5)	1368 (4)	845 (6)
C52	704 (5)	723 (4)	810 (6)	C53	1513 (6)	512 (5)	866 (7)
C54	2141 (6)	948 (5)	974 (7)	C55	1994 (6)	1579 (4)	1019 (6)
C56	1178 (5)	1802 (4)	957 (6)	C61	−1086 (4)	2744 (4)	4140 (5)
C62	−1254 (5)	2439 (4)	4981 (6)	C63	−875 (6)	2658 (4)	5962 (7)
C64	−335 (6)	3150 (4)	6087 (7)	C65	−155 (6)	3457 (5)	5274 (7)
C66	−526 (5)	3248 (4)	4299 (6)	C71	−2565 (4)	2935 (3)	2608 (5)
C72	−2817 (5)	3289 (4)	3348 (6)	C73	−3576 (5)	3614 (4)	3155 (7)
C74	−4097 (6)	3586 (4)	2235 (6)	C75	−3881 (5)	3249 (4)	1478 (7)
C76	−3107 (5)	2934 (4)	1652 (6)				
			Molecule 6				
Rh	729 (1)	2566 (1)	1678 (1)	Hf	−1390 (1)	1313 (1)	2146 (1)
P1	−468 (2)	3550 (1)	995 (2)	P2	−552 (1)	1655 (1)	793 (2)
P3	−1576 (1)	2489 (1)	2827 (2)	O	934 (5)	2475 (3)	3243 (6)
C	314 (6)	2521 (4)	2649 (8)	C1	79 (7)	1000 (5)	3056 (8)
C2	−283 (6)	1304 (5)	3771 (8)	C3	−942 (7)	922 (5)	3926 (8)
C4	−978 (7)	382 (6)	3327 (8)	C5	−367 (7)	429 (5)	2784 (8)
C6	−2961 (6)	1373 (5)	1640 (7)	C7	−2745 (6)	754 (5)	2028 (8)
C8	−2359 (7)	437 (6)	1342 (8)	C9	−2316 (7)	850 (5)	582 (8)
C10	−2681 (6)	1438 (5)	742 (8)	C11	−54 (5)	4170 (4)	1937 (6)
C12	699 (6)	4075 (5)	2633 (7)	C13	990 (8)	4501 (6)	3401 (9)
C14	567 (9)	5041 (7)	3488 (11)	C15	−173 (10)	5157 (8)	2771 (12)
C16	−468 (8)	4746 (6)	1993 (9)	C21	310 (6)	3546 (5)	225 (7)
C22	271 (7)	3064 (5)	−498 (8)	C23	876 (7)	3019 (5)	−1050 (9)
C24	1519 (7)	3446 (6)	−916 (9)	C25	1555 (8)	3929 (6)	−236 (9)
C26	969 (7)	3990 (6)	338 (9)	C31	−1364 (6)	3947 (4)	137 (7)
C32	−2112 (7)	3985 (5)	410 (9)	C33	−2813 (8)	4273 (6)	−185 (9)
C34	−2759 (9)	4535 (7)	−1095 (10)	C35	−2022 (8)	4506 (6)	−1393 (10)
C36	−1338 (7)	4235 (5)	−781 (8)	C41	−1049 (5)	1606 (4)	−578 (7)
C42	−838 (7)	1145 (5)	−1210 (8)	C43	−1264 (8)	1072 (6)	−2203 (9)
C44	−1905 (8)	1469 (6)	−2600 (9)	C45	−2129 (8)	1953 (6)	−2003 (9)
C46	−1681 (7)	2009 (5)	−1021 (8)	C51	517 (6)	1372 (4)	848 (7)
C52	712 (7)	715 (5)	813 (7)	C53	1509 (7)	520 (6)	868 (8)
C54	2138 (8)	948 (6)	958 (9)	C55	1988 (7)	1573 (5)	1011 (8)
C56	1186 (6)	1793 (5)	973 (7)	C61	−1089 (6)	2740 (4)	4133 (7)
C62	−1261 (6)	2437 (5)	4977 (7)	C63	−880 (7)	2643 (5)	5952 (8)
C64	−334 (7)	3142 (5)	6088 (9)	C65	−145 (7)	3442 (6)	5281 (9)
C66	−523 (6)	3247 (5)	4295 (8)	C71	−2573 (6)	2939 (4)	2592 (7)
C72	−2821 (6)	3279 (5)	3355 (8)	C73	−3582 (8)	3608 (5)	3201 (10)
C74	−4114 (8)	3589 (5)	2230 (9)	C75	−3885 (7)	3259 (5)	1471 (9)
C76	−3131 (6)	2945 (5)	1651 (7)				

[a] Multiplied by 10^4.

sponding doublet of doublets and doublet of triplets. These signals and their intensities are consistent with two magnetically equivalent bridging phosphido groups that couple to the phosphorus of the phosphine bound to the late metal. The ^1H NMR spectra of complexes **2–7**, show the expected resonances for the phosphido and phosphine substituents. Two resonances arise from the Cp protons, consistent with the chemical inequivalence of the Cp groups. In the high-field region (−12 to −13 ppm) the ^1H resonances attributable to the hydrides were observed. Coupling of the hydride to the phosphorus nuclei and to the Rh in the case of the Rh complexes is apparent. ^{31}P NMR experiments in which continuous wave, selective decoupling was employed allowed the observation of phosphorus to hydride coupling (Figure 1). In this way, all $|J(P-H)|$ values as well as $|J(Rh-H)|$ values were unambiguously determined. These NMR data are consistent with a pseudo-trigonal-bipyramidal geometry about Ir or Rh, in which the three phosphorus nuclei occupy the equatorial plane. Axial ligation by hydride is suggested

Table III. Selected Bond Distances and Angles

	Molecule 2		
	Distances (Å)		
	Rh–Zr 2.980 (1)		
Rh–P1	2.341 (2)	Rh–P2	2.313 (2)
Rh–P3	2.320 (3)	Rh–C	1.90 (1)
Zr–P2	2.671 (2)	Zr–P3	2.698 (2)
Zr–C1	2.538 (8)	Zr–C2	2.542 (8)
Zr–C3	2.506 (9)	Zr–C4	2.518 (9)
Zr–C5	2.50 (1)	Zr–C6	2.527 (8)
Zr–C7	2.499 (8)	Zr–C8	2.493 (9)
Zr–C9	2.516 (8)	Zr–C10	2.528 (8)
P1–C11	1.816 (7)	P1–C21	1.841 (8)
P1–C31	1.831 (8)	P2–C41	1.843 (8)
P2–C51	1.830 (7)	P3–C61	1.844 (7)
P3–C71	1.834 (7)	C–O	1.15 (1)
	Angles (deg)		
Zr–Rh–P1	167.0 (1)	Zr–Rh–P2	59.0 (1)
P1–Rh–P2	117.1 (1)	Zr–Rh–P3	59.7 (1)
P1–Rh–P3	120.9 (1)	P2–Rh–P3	118.3 (1)
Zr–Rh–C	96.6 (3)	P1–Rh–C	96.3 (3)
P2–Rh–C	96.7 (3)	P3–Rh–C	96.1 (3)
Rh–Zr–P2	47.9 (1)	Rh–Zr–P3	47.9 (1)
P2–Zr–P3	95.6 (1)	Rh–P2–Zr	73.0 (1)
Rh–P3–Zr	72.4 (1)	Rh–C–O	178.1 (7)
	Molecule 6		
	Distances (Å)		
	Rh–Hf 2.964 (1)		
Rh–P1	2.339 (2)	Rh–P2	2.309 (2)
Rh–P3	2.325 (2)	Rh–C	1.90 (1)
Hf–P2	2.640 (2)	Hf–P3	2.672 (2)
Hf–C1	2.52 (1)	Hf–C2	2.51 (1)
Hf–C3	2.49 (1)	Hf–C4	2.51 (1)
Hf–C5	2.51 (1)	Hf–C6	2.50 (1)
Hf–C7	2.48 (1)	Hf–C8	2.50 (1)
Hf–C9	2.50 (1)	Hf–C10	2.51 (1)
P1–C11	1.83 (1)	P1–C21	1.83 (1)
P1–C31	1.85 (1)	P2–C41	1.85 (1)
P2–C51	1.84 (1)	P3–C61	1.84 (1)
P3–C71	1.85 (1)	C–O	1.14 (1)
	Angles (deg)		
Hf–Rh–P1	167.1 (1)	Hf–Rh–P2	58.5 (1)
P1–Rh–P2	117.6 (1)	Hf–Rh–P3	59.2 (1)
P1–Rh–P3	121.4 (1)	P2–Rh–P3	117.4 (1)
Hf–Rh–C	96.9 (3)	P1–Rh–C	95.8 (3)
P2–Rh–C	96.7 (3)	P3–Rh–C	96.4 (3)
Rh–Hf–P2	48.3 (1)	Rh–Hf–P3	48.4 (1)
P2–Hf–P3	96.4 (1)	Rh–P2–Hf	73.2 (1)
Rh–P3–Hf	72.4 (1)	Rh–C–O	177.8 (8)

by the relatively small value of $|J(\text{Rh–H})|$. The M′–H and CO stretching frequencies are observed in the IR spectrum in ranges similar to those observed in the monometallic Ir and Rh starting materials. This suggests that the coordination spheres of the late metals are completed by CO in the remaining axial position. The dissymmetric axial ligation places each of the Cp groups on the early metal in positions cis to one of the two axial ligands on the late metal, thus accounting for the the observed inequivalence of the Cp groups in the ^{1}H NMR spectra. This interpretation of the NMR data is consistent with the results of the structural studies (*vide infra*).

Structure Descriptions. An X-ray crystallographic study of **2** revealed that the crystals are made up of monoclinic unit cells each containing four discrete molecules. The closest approach between any two of these molecules is 2.282 Å (H9···H53). Selected bond distances and angles are given in Table III. An ORTEP drawing of the molecule is given in Figure 2. The coordination geometry of the Zr is pseudotetrahedral. Two π-bonded cyclopentadienyl rings and two phosphido groups comprise the coordination sphere of the Zr. The Zr–C distances average 2.52 (2) Å which is typical.[22,23,31] The Zr–P distances are 2.671 (2) and 2.698 (2) Å. This is significantly longer than those observed for $Cp_2Zr(\mu\text{-}PPh_2)_2Mo(CO)_4$ (2.630 (1) and 2.631 (1) Å[31]) and $Cp_2Zr(\mu\text{-}PPh_2)W(CO)_4$ (2.631 (3) and 2.619 (3) Å[22]). The coordination sphere of the Rh is pseudo-trigonal-bipyramidal. The equatorial plane of the trigonal bipyranid (tbp) contains the two bridging phosphido groups and a PPh_3. The P–Rh–P angles range from 117.1 (1) to 120.9 (1)° consistent with a tbp geometry. The carbonyl group occupies a position that is essentially axial to the plane of the three phosphorus nuclei. The hydride was not located in the crystallographic study; however, it presumably occupies the axial position trans to the CO group. The Rh–P distances for the μ-PPh_2 groups are slightly shorter than the Rh–PPh_3 distance. This is consistent with the greater basicity of the μ-PPh_2 groups. The Rh–C distance is typical.[45]

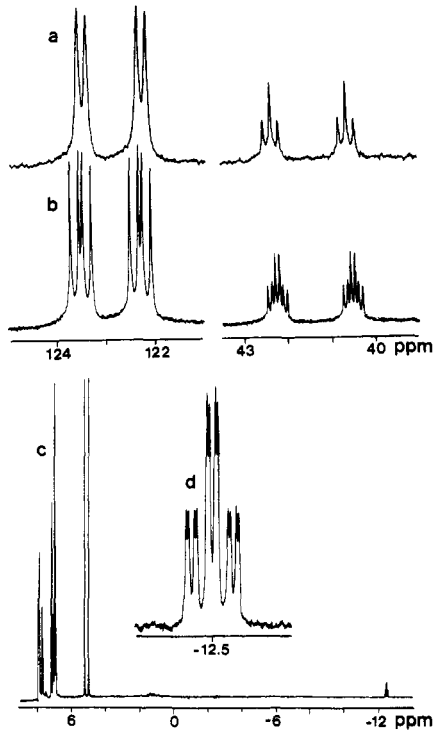

Figure 1. (a) $^{31}P\{^1H\}$ NMR spectrum of **6**. (b) ^{31}P NMR spectrum of **6** in which CW decoupling is used to yield only P–hydride coupling. (c) ^1H NMR spectrum of **6**. (d) The hydride region of the ^1H NMR spectrum of **6**.

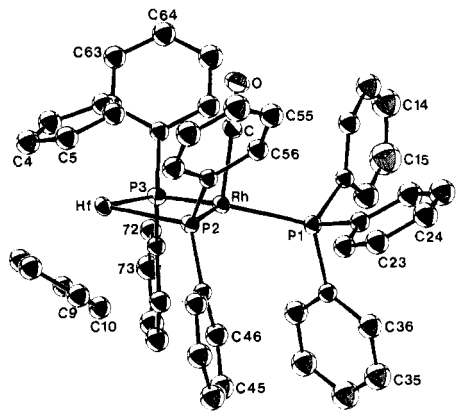

Figure 2. ORTEP drawing of **6**. Hydrogen atoms are omitted for clarity; 30% thermal ellipsoids are shown. Note that the labeling scheme for **2** is identical with that shown for **6** with the replacement of Hf for Zr.

(45) LaPlaca, S. J.; Ibers, J. A. *Acta Crystallogr.* **1965**, *18*, 511.

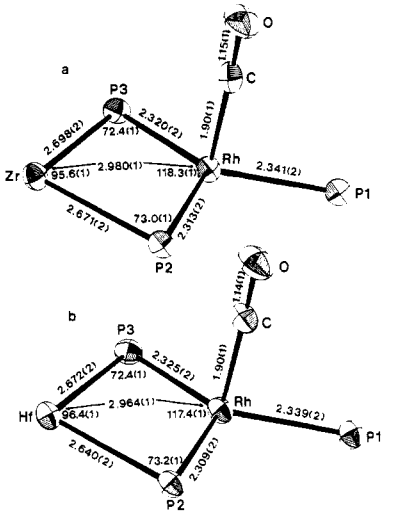

Figure 3. ORTEP drawings of the cores of molecules **2** and **6**. The distances are given in Å and the angles in deg.

An X-ray study of **6** showed that it is isostructural to **2**. The closest approach between molecules in the unit cell is 2.321 Å (H9···H53). Selected bond distances and angles are given in Table III. Hf–C distances are typical.[23] The Hf–P distances (2.672 (2) and 2.640 (2) Å) in **6** are shorter than the corresponding Zr–P distances of **2** (2.698 (2) and 2.671 (2) Å) and significantly longer than the Zr–P distances found in $Cp_2Hf(\mu\text{-}PEt_2)_2Mo(CO)_4$ (2.592 (1), 2.596 (1) Å[23]). Rh–P and Rh–C distances in **6** do not differ significantly from those found in **2**.

The structural details of the $MP_2Rh(CO)P$ cores for **2** and **6** are shown in Figure 3. The MP_2Rh cores are not planar rather they are "butterfly" shaped. The angles between the MP_2 plane and the RhP_2 plane are 9.94° and 9.73° for **2** and **6** respectively. The M–P–Rh angles in **2** and **6** are similar, being in the range of 72.4–73.2°. Angles of less than 80° at bridging atoms have been previously used as evidence for metal–metal interactions.[46] The P–Rh–P angles are 118.3 (1) and 117.4 (1)° for **2** and **6**, respectively. The P–M–P angles at either Zr or Hf are 95.6 (1) and 96.4 (1)°. The Zr–Rh distance in **2** is 2.980 (1) Å while the Hf–Rh distance is 2.964 (1) Å. These distances are slightly greater than the metal–metal separation seen in $Cp_2Hf(\mu\text{-}PPh_2)_2PdPPh_3$ (2.896 Å).[47] The M–Rh distances, the angles about the cores, and the "butterfly" nature of the MP_2Rh cores suggest the presence of metal–metal interactions between the d^8 Rh(I) center and the d^0 Zr(IV) or Hf(IV) center in **2** and **6**. In addition, the relatively long Zr–P and Hf–P bond lengths in **2** and **6** compared to those seen in related d^6–d^0 heterobimetallics[22,23] are consistent with donation of electron density to the early metal center from the d^8 Rh center. This suggests the possibility of the bonding mode represented by **11**. We have previously described chemical and

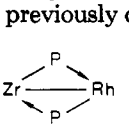

11

structural evidence for such dative interactions between an electron-rich and electron-deficient metal center in other early/late heterobimetallic systems.[31-37] Molecular orbital calculations support the presence of such dative interactions in related heterobimetallics.[12,38]

Reactivity. The reactions of **2** with PEt_3 and PCy_3 were monitored by $^{31}P\{^1H\}$ NMR spectroscopy. The spectra show established equilibria in which the more basic trialkylphosphine exchanges with the PPh_3 bound to the Rh. Thus resonances arising from **2**, free PPh_3, free trialkylphosphine, and the complex $Cp_2Zr(\mu\text{-}PPh_2)_2RhH(CO)PR_3$ (R = Et (**8**) or R = Cy (**9**)) are observed. ^{31}P NMR chemical shifts and phosphorus–phosphorus coupling constants for **8** and **9** suggest a similar geometry to that seen in **2**. The equilibrium constants for these exchanges processes (eq 1) were calculated on the basis of the inte-

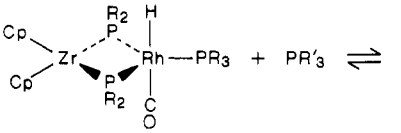

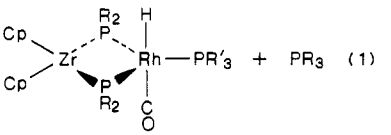

grations of the $^{31}P\{^1H\}$ NMR spectra. Substitution occurred to a greater extent with PEt_3 (K_{eq} = [**8**][PPh_3]/[**2**][PEt_3] ≃ 65) than with PCy_3 (K_{eq} = [**9**][PPh_3]/[**2**][PCy_3] ≃ 1.6), clearly reflecting the relative steric bulk of the two ligands. Similar effects of steric bulk on phosphine exchange reactions were observed for $Cp_2Zr(\mu\text{-}PPh_2)_2PtPPh_3$.[32]

Carbon monoxide also reacts with **2**. The $^{31}P\{^1H\}$ NMR spectrum of the reaction mixture under 1 atm of CO and 25 °C showed an equilibrium between **2**, free PPh_3, and a product, formulated as $Cp_2Zr(\mu\text{-}PPh_2)_2RhH(CO)_2$, (**10**).

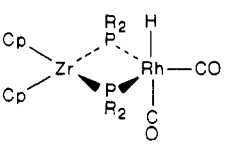

10

The $^{31}P\{^1H\}$ NMR spectrum of **10** consists of a doublet at 128 ppm, indicative of chemically equivalent phosphido groups. Continuous-wave selective decoupling experiments were performed as described for **2**–**7**. The results of these experiments together with the ^1H NMR resonance at −12.39 ppm and the IR stretching frequency at 2017 cm^{-1} confirmed the presence of a hydride on Rh. Resonances attributable to the protons of the Cp and phenyl groups as well as the ν_{CO} values observed in the IR at 1975 and 1933 cm^{-1} are consistent with the proposed formulation. The spectral data suggest a molecular geometry similar to **2**, in which CO has replaced PPh_3. The equilibrium constant (K_{eq} = [**10**][PPh_3]/[**2**] (1 atm of CO)), calculated from $^{31}P\{^1H\}$ NMR spectrum integration, is 33. Attempts to isolate **10** free of residual **2** and PPh_3 were not successful.

Attempted reactions of **2** with H_2 were performed at 1 atm of H_2 and 25 °C for 2–24 h. No reaction was seen under these conditions. Similarly, mixtures of **2** with 1-hexene showed no evidence of reaction even in the presence of large excesses of olefin. In contrast, reactions with dimethyl acetylenedicarboxylate or carbon disulfide led to decomposition of **2**, yielding products which are as yet uncharacterized.

Catalysis. The hydroformylation of 1-hexene was catalyzed by using either **2** or $RhH(CO)(PPh_3)_3$ as the catalyst precursors. The reactions were done at either 25 or 50 °C under 1 atm of a 50:50 CO/H_2 mixture. In all cases, the catalyst precursor was present in 1 mol %. The

(46) Davies, G. R.; Kilbourn, B. T. *J. Chem. Soc. A.* **1971**, 87.
(47) Baker, R. T., private communication.

Table IV. Product Distribution for the Hydroformylation of 1-Hexene

cat. precursor[a]	% reaction	% *n*-heptanal	% 2-methylhexanal
$RhH(CO)(PPh_3)_3$	99	67	30
2	91	81	5
2[b]	89	80	5
2 + 10× excess PPh_3	22	20	1

[a] Except where otherwise stated the reactions were performed at 25 °C and were monitored for 100 h. [b] This reaction was performed at 50 °C and monitored for 60 h.

reactions were monitored by GLC and GLC–MS. The product yields and distributions are reported in Table IV. After 100 h at 25 °C, the reaction employing **2** as the catalyst precursor consumed about 90% of the 1-hexene. In contrast, 99% of the 1-hexene was consumed when $RhH(CO)(PPh_3)_3$ was used as the catalyst precursor after only about 12–15 h. Thus, during the initial 10–15 h, the monometallic Rh catalyst reacted at a rate that is about 6.3 times greater than the heterobimetallic species. However, the overall yield of *n*-heptanal was greater (80% vs. 67%) when the heterobimetallic catalyst precursor **2** was used while the yield of 2-methylhexanal was substantially lower. In all cases, small amounts of the hydrogenation (hexane) and olefin isomerization (2-hexene) products were also observed.

The increase in selectivity for the terminal aldehyde when the heterobimetallic catalyst precursor is used is reflected in the greater linear:branched aldehyde ratio (16:1 vs. 2:1). Isomerization of the product *n*-aldehyde by the monometallic Rh catalyst has been previously observed.[48-52] This is evident in the present data from the gradual decrease in the amount of *n*-heptanal after the first 20 h of reaction (Figure 4). No evidence of this isomerization process is observed when the heterobimetallic catalyst precursor is used. The reasons for this are not clear, but it may be a result of the geometrical constraints imposed by the chelating nature of the Zr–diphosphide metalloligand.

When the heterobimetallic catalyst precursor is used, an increase in the temperature at which the catalysis is performed results in a 2.6-fold increase in the rate of formation of the products; however, the product distribution is unchanged. Addition of a tenfold excess of PPh_3 inhibits the reaction, reducing the rate of hydroformylation by a factor of 4. This implies phosphine dissociation from Rh is involved either in the mechanism of catalysis or in the generation of the catalyst.

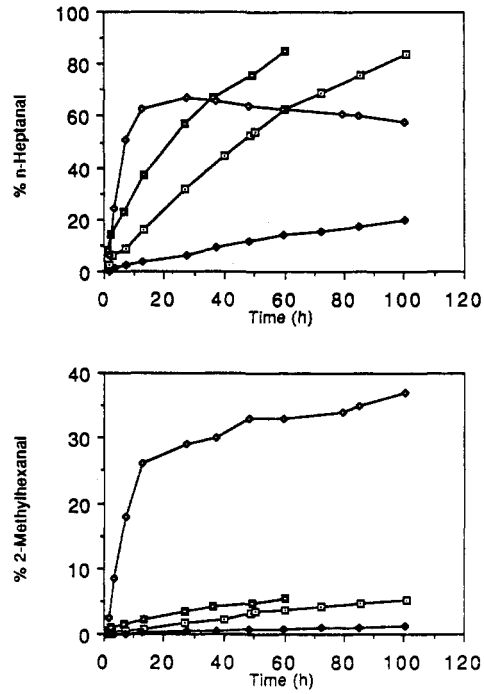

Figure 4. The products of catalytic hydroformylation of 1-hexene. (a) Plot showing the production of *n*-heptanal as a function of time. (b) Plot showing the production of 2-methylhexanal as a function of time. In both plots, ◘ refers to the catalysis at 25 °C in which $RhH(CO)(PPh_3)_3$ was used as the catalyst precursor, ♦ to the case where **2** was used as the catalyst precursor at 25 °C, □ to **2** at 50 °C, and ◊ to **2** in the presence of a tenfold excess of PPh_3 at 25 °C.

The nature of the catalyst in the cases where the heterobimetallic precursor is employed is not fully understood. However, **2** can be recovered virtually quantitatively from the reaction mixture following catalysis. Furthermore, the substitution reactions described above show that the integrity of the heterobimetallic is maintained even in the presence of excess donor ligands. These facts suggest but do not confirm that the actual catalyst is a heterobimetallic. Attempts to clarify the nature of the catalyst and its mechanism of action are in progress.

Acknowledgment. NSERC of Canada is thanked for financial support of this work. L.G. is grateful for the award of a NSERC of Canada Postgraduate Scholarship.

Registry No. **2**, 112896-11-4; **3**, 112896-12-5; **4**, 112896-13-6; **5**, 112896-14-7; **6**, 112896-15-8; **7**, 112896-16-9; **8**, 112896-17-0; **9**, 112896-18-1; **10**, 112896-19-2; $Cp_2Zr(PPh_2)_2$, 86013-25-4; $RhH(CO)(PPh_3)_3$, 17185-29-4; $Cp_2Hf(PPh_2)_2$, 86013-28-7; $Cp_2Zr(PCy_2)_2$, 86013-24-3; $Cp_2Hf(PCy_2)_2$, 86013-27-6; $IrH(CO)(PPh_3)_3$, 33541-67-2; 1-hexene, 592-41-6.

Supplementary Material Available: Thermal parameters (Table S1), hydrogen atom parameters (Table S2), and bond distances and angles associated with the phenyl and cyclopentadienyl rings (Table S3) (12 pages); values of $10|F_o|$ and $10|F_c|$ (Table S4) (31 pages). Ordering information is given on any current masthead page.

(48) Evans, D.; Osborn, J. A.; Wilkinson, G. *J. Chem. Soc. A* **1968**, 3133.
(49) Pruett, R. L.; Smith, J. A. *J. Org. Chem.* **1969**, *34*, 327.
(50) Evans, D.; Yagupsky, G.; Wilkinson, G. *J. Chem. Soc. A* **1968**, 2660.
(51) Yagupsky, M.; Brown, C. K.; Yagupsky, G.; Wilkinson, G. *J. Chem. Soc. A* **1970**, 937.
(52) Yagupsky, G.; Brown, C. K.; Wikinson, G. *J. Chem. Soc. A* **1970**, 1392.
(53) Lukehart, C. M. *Fundamental Transition Metal Organometallic Chemistry*; Brooks/Cole: Monterey, CA, 1984.